3D Simulations of Ultra-Small MOSFETs: The Role of the Short Range Coulomb Interactions and Discrete Impurities on Device Terminal Characteristics*

W. J. Gross,[1] D. Vasileska[2] and D. K. Ferry[2]

[1]Intel Corp., Chandler, AZ 85226
e-mail: william.j.gross.jr@intel.com, phone: (480) 554-5623

[2]Department of Electrical Engineering, Arizona State University
Tempe, AZ 85287-5706, USA
e-mail: vasilesk@imap2.asu.edu, ferry@asu.edu

ABSTRACT

We have developed a three-dimensional particle based simulator with a coupled molecular dynamics routine that avoids the "double-counting" of the long-range portion of the Coulomb force. As opposed to drift-diffusion based simulators, the Monte Carlo simulator can accurately model high field transport in semiconductor devices, while enabling the real-space treatment of the interactions, including multi-ion and particle contributions, through the coupled molecular dynamics scheme. The inclusion of the electron-electron and electron-ion interactions was shown to play an important role in device simulations. The drain current for MOSFET devices was significantly decreased when the Coulomb forces were added. Using this simulator, random dopant ions in the channel have shown to create fluctuations in the drain current of deep sub-micron MOSFETS as well as fluctuations in the device threshold voltage.

Keywords: ultra-small MOSFETs, discrete impurity effects, threshold voltage fluctuations, high-field transport.

1. INTRODUCTION

Advances in lithography have driven device dimensions to the deep-submicrometer range, where gate lengths are drawn at 0.25 μm and below. Currently, 0.18 μm is the industry's state-of-the-art process technology and 0.1 μm devices are in preproduction. Via experiments and numerical simulations, it is now recognized that the atomistic nature of the impurity atoms in the active region of these ultra-small devices of the future will lead to significant fluctuations in the device threshold voltage and the terminal device characteristics. For better insight of the importance of this issue, let us consider a prototypical MOSFET with 0.07 μm channel length, 0.07 μm channel width and channel doping of 10^{18} cm^{-3}. The number of dopant atoms in the depletion region of this device is on the order of several hundreds, and well below 100 in its active region. With such a small number of the impurity atoms, the local variations in the "doping concentration" across the channel will become a significant factor in determining the threshold voltage, mobility and drain current characteristics. This, in turn, can cause considerable problems for circuit design, especially for circuits in which the devices must be well matched, such as operational amplifiers and static random access memories.

Experimental studies by Mizuno and co-workers [1] have shown that the threshold voltage standard deviation is inversely proportional to the square-root of the area and is proportional to the oxide thickness and the fourth-root of the average doping in the channel region of the device. They found that the statistical variation of the channel dopant number accounts for about 60% of the experimentally derived threshold voltage fluctuations. In a later study, Mizuno [2] also found that the lateral and vertical arrangement of ions produces variations in the threshold voltage dependence upon the drain and substrate biases. Quite recently, Horstmann and his co-workers [3], who investigated the global and local matching of sub-100 nm NMOS- and PMOS-transistors, confirmed the law of area proposed in [1]. The empirical analytical expression by Mizuno was generalized by Stolk *et al*. [4] by taking into account the finite thickness of the inversion layer, depth-distribution of charges in the depletion layer and the influence of the source and drain dopant distributions and depletion regions.

Numerical drift-diffusion and hydrodynamic simulations of devices with 10-30 random dopant distributions [4-9] have also confirmed the existence of the fluctuations in the threshold voltage in ultra-small devices. 2D [10] and 3D [11,12] Monte Carlo particle-based simulations have also been carried out. An important observation was made by Vasileska, Gross and Ferry [9], who showed that there is a significant correlation between the threshold voltage shifts and the actual position of the impurity atoms. A rather systematic analysis of the random dopant induced threshold voltage fluctuations in ultra-small MOSFETs was carried out by Asenov [13] using 3D drift-diffusion device simulations and confirming previous results. Recent simulation experiments by Asenov and Saini [14] show that the random dopant induced effects are significantly suppressed in MOSFETs with a δ-doped channel.

However, the majority of the above-mentioned simulation experiments, except [11,12], utilized 2D or 3D device simulators, in which the "discreteness" of the ions is only accounted for through the charge assignment to the mesh nodes. There, the long-range portion of the electron-ion forces is inherent in the mesh force and is found from the solution of Poisson's equation. The short-range portion of these interactions is, thus, completely ignored. Our group showed recently that proper inclusion of the short-range electron-electron and electron-ion interactions is needed for accurate description of the doping dependence of the low-field electron mobility [15], thermalization of the carriers at the drain end of the device [11,12], and proper description of the drain current saturation characteristics [16]. Description of our coupled EMC-MD routine, that prevents the double-counting of the force is given in [15]. A very detailed description of our 3D EMC -MD simulator can be found in Refs. [11,12,15,16]. Here, in section 2 of the paper, we discuss the role of the statistical dopant fluctuations upon device threshold voltage fluctuations for devices with different channel width and substrate doping. In section 3, we discuss discrete impurity effects on device terminal characteristics at high fields. Conclusions derived from the work presented here are given in section 4.

2. THRESHOLD VOLTAGE FLUCTUATIONS

Statistical threshold voltage fluctuations due to the discrete impurity effects were studied using samples of random dopant distibutions in the channel for several different device sizes. For each device size, a statistical sample of 30 devices with identical geometry but different distribution of impurity atoms was simulated. The average source, drain, and bulk impurity concentrations were exactly the same for a given device type. The number of dopant atoms in the channel region, defined as the region between the source and drain down to the depth of the source and drain junctions, was chosen based upon a Poisson distribution around the expected number of dopant atoms. It this region, the atoms were "implanted" at a randomly chosen site using the technique described in [8].

It is important to point out that, since the number of particles in the channel is relatively small (on the order of 10 to 100 electrons, depending upon device size) accurate current measurements are difficult. To avoid this problem, we defined the threshold voltage being equal to the gate voltage for which there are 10^{12} particles per square centimeter under the gate. Using a constant charge density method ensured that the device was in inversion while reducing the noise in the measurement. It should be noted that this measurement technique yields a threshold voltage V_T that is higher than the one derived from the current measurement because the device is truly inverted.

Scatter plots of the threshold voltage versus number of channel dopant atoms for the statistical sample of 30 devices with channel length $L_G = 50$ nm, junction depth $X_J = 25$ nm, average channel doping $N_A = 5\times10^{18}$ cm^{-3} and oxide thickness $T_{OX} = 2$ nm are shown in Figs. 1(a-c). The only difference between these device sets is the width of the device, which was set to 35, 70 and 100 nm, respectively. Due to the assumed zero-field boundary conditions along the width direction, there is no width dependence of the threshold voltage, and the average V_T for each device group is roughly 800 mV. This result also confirms that the constant surface concentration technique is a stable measurement for the threshold voltage. From the results shown, it is easily seen that the smaller device size results in higher fluctuations in the V_T, as expected. More details on the variation of the standard deviation of the threshold voltage upon the oxide thickness and average substrate doping can be found in [12].

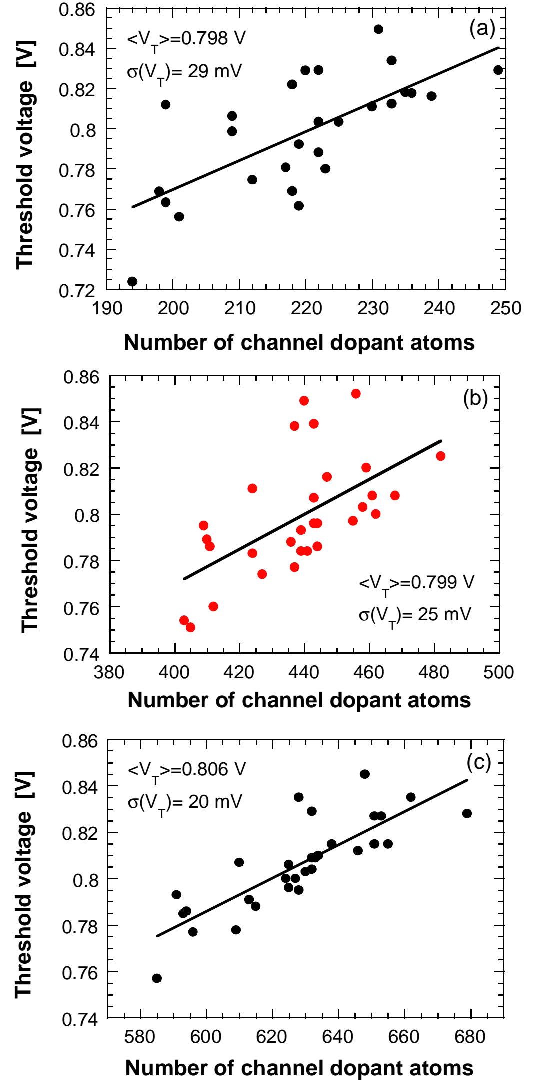

Figure 1. Threshold voltage versus number of channel dopant atoms for device with (a) $W_G = 35$ nm, (b) $W_G = 70$ nm, and (c) $W_G = 100$ nm.

It is important to note that the simulation time needed to make a stable V_T measurement was 12 to 36 hours per device. In running these simulations, the number of devices in our ensembles was chosen to be statistically significant without needing an excessive amount of CPU time. To further investigate the device fluctuations, a sample of 15 devices was selected from an ensemble of 1000 doping configurations for devices with L_G = 50 nm, W_G = 35 nm, junction depth X_J = 25 nm, average channel doping N_A = 5×10^{18} cm^{-3} and oxide thickness T_{OX} = 3 nm. Five devices were taken from each end of the distribution, and five devices were taken from the center.

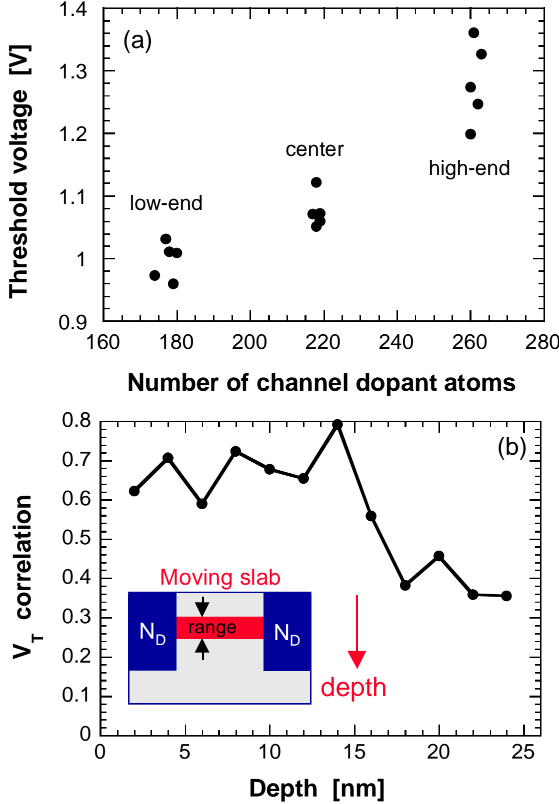

Figure 2. (a) Threshold voltage versus number of dopant atoms in channel for 15 selected devices from the statistical ensemble of 1000 devices with T_{OX} = 3 nm. (b) Correlation of the threshold voltage to number of dopant atoms in a 10 nm range at various depths beneath the channel.

A V_T scatter plot for the group of 5 devices taken from the low-end, center and the high-end of the statistical sample of 1000 devices is shown in Figure 2(a). The variations in the number of channel dopant atoms produced an effective doping concentration ranging from 4.2×10^{18} cm^{-3} to 6.2×10^{18} cm^{-3} for the devices at the ends of the distribution. Looking at the 3 groups of 5 devices, there is a strong correlation between the number of dopant atoms and the average threshold voltage. The devices at the higher end of the distribution have an average V_T that is approximately 300 mV higher than the corresponding one for the devices at the low end. This shift is due to the difference in the effective doping between these two sets of devices. However, it does not completely account for the total threshold voltage range of 400 mV seen between the device types. Even within the 5 devices at the high end of the dopant number distribution, there is a V_T fluctuation of ~160 mV. This deviation is due to the arrangement of the atoms, since the number of dopant atoms for these devices are nearly the same. To justify this, the threshold voltage was correlated to the number of dopant atoms at a given depth that fall in a 10 nm range. Figure 2(b) shows the square of the correlation coefficient versus depth. Down to 15 nm from the semiconductor/oxide interface, there is a strong correlation between the threshold voltage V_T and the number of dopant atoms that fall in the moving slab region schematically shown in the inset of Fig. 2(b). The correlation falls rapidly between 15 and 18 nm depth, and then stays fairly constant. Beyond 18 nm, the correlation remains strong due to the dependence of the average threshold voltage on the doping concentration. Hence, the dopant atoms in the top 18 nm of the channel significantly affect the magnitude of V_T.

3. DRAIN SATURATION CURRENT

In Figure 3(a), the drain current is plotted versus the number of channel dopant atoms for the statistical sample of 15 devices from Fig. 2. Each device was simulated for 4 ps, with the gate voltage set to 1.5 V and the drain voltage set to 1.0 V. The drain current was measured by averaging the velocity of electrons in the channel over the last 2.4 ps of the simulation. It is important to note that at these bias conditions, the devices were in the saturation region of the I_D-V_G curve, but were not velocity saturated. As the number of channel dopant atoms increases, the drain current decreases due to the increase in the V_T.

Besides affecting the threshold voltage, the impurity distribution in the channel plays fundamental role in determining the mobility of the channel electrons. Figure 3(b) shows a plot of the average velocity of channel electrons versus the number of dopant atoms in the channel. As expected, the velocity decreases as the number of dopant atoms increases due to increased ionized impurity scattering. At the low end of the dopant number distribution, the average electron velocity is roughly the same for each dopant configuration. However, the fluctuation in the electron velocity increases with the number of dopant atoms, with a 3× spread in the velocity seen for the devices at the high dopant number extreme.

The average electron velocity and device drain current characteristics were correlated to the number of dopant atoms in a 10 nm range at various depths. Figure 3(c) shows a plot of the square of the correlation coefficient versus depth (beneath the semiconductor/oxide interface). The correlation to the electron velocity is very high for the first 6 nm, and steadily decreases up to 18 nm depth, be-

yond which the correlation is nearly zero. It appears that only the dopant atoms in the first 6-10 nm from the semiconductor/oxide interface have significant effect on the velocity. This is reinforced by the fact that the correlation nearly goes to zero at a depth of 18 nm, as opposed to the threshold voltage correlation, which remains fairly high at a larger depth. The correlation of the drain current to the number of dopant atoms is also high near the surface, but the drop-off is not as steep as the velocity correlation. Beyond 18 nm depth, the correlation of the drain current is non-zero due to the correlation of the threshold voltage to the number of dopant atoms (see previous discussion).

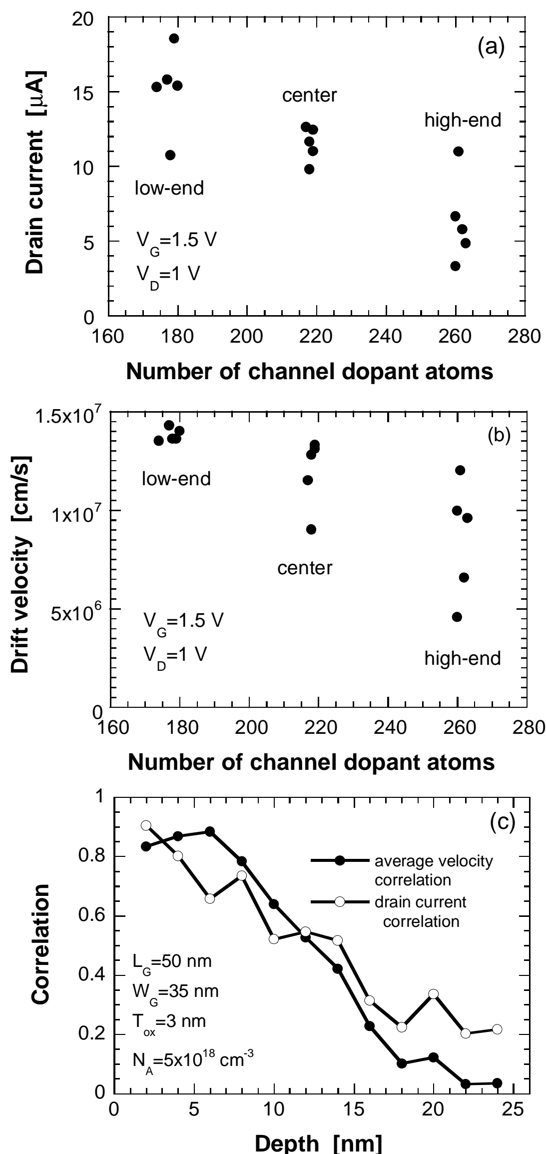

Figure 3. (a) Drain current versus the number of channel dopant atoms. (b) Average velocity of channel electrons versus the number of channel dopant atoms. (c) Correlation of the drain current and average electron velocity to the number of dopant atoms within a 10 nm range at various depths beneath the channel.

4. CONCLUSIONS

Fluctuations in the threshold voltage in ultra-small devices were shown to be due to the number and the actual position of the dopant atoms in the device active region. These results concur with previous experiments using drift-diffusion based simulators. Trends in the V_T fluctuations versus device width, substrate doping, and oxide thickness were all shown to be in agreement with analytical models. Correlation of the threshold voltage to the number of dopant atoms in a 10nm range at various depths showed that the atoms in the top 15-20 nm beneath the channel are the most significant. Similar correlation with the average drift velocity showed that only the atoms in the top 8 nm have an impact on the electron drift velocity.

REFERENCES

* One of the authors (DV) would like to acknowledge the financial support from ONR under Contract No. N00014-99-1-0318 and from NSF under Contract No. ECS-9875051.

[1] T. Mizuno, J. Okamura and A. Toriumi, IEEE Trans. Electron Devices, vol. 41, 2216 (1994).

[2] T. Mizuno, Jpn. J. Appl. Phys., vol. 35, 842 (1996).

[3] J. T. Horstmann, U. Hilleringmann and K. F. Goser, IEEE Trans. Electron Devices, vol. 45, 299 (1998).

[4] P. A. Stolk, F. P. Widdershoven and D. B. M. Klaassen, IEEE Trans. Electron Devices, vol. 45, 1960 (1998).

[5] K. Nishinohara, N. Shigyo and T. Wada, IEEE Trans. Electron Devices, vol. 39, 634 (1992).

[6] J.-R. Zhou and D.K. Ferry, IEEE Comput. Science and Eng., vol. 2, 30 (1995).

[7] H.-S. Wong and Y. Taur, IEDM Tech. Dig., 705 (1993).

[8] D. Vasileska, W. J. Gross, V. Kafedziski and D. K. Ferry, VLSI Design, vol. 8, Nos. 1-4, 301 (1998).

[9] D. Vasileska, W. J. Gross and D. K. Ferry, Extended Abstracts IWCE-6, Osaka 1998, IEEE Cat. No. 98EX116, 259.

[10] X. Tang, V. K. De and J. D. Meindl, IEEE Trans. on VLSI Systems, vol. 5, 369 (1997).

[11] W. J. Gross, D. Vasileska, and D. K. Ferry, VLSI Design (special issue), in press.

[12] W. J. Gross, D. Vasileska, and D. K. Ferry, Superlattices and Microstructures, submitted for publication.

[13] A. Asenov, IEEE Trans. Electron Dev., vol. 45, 2505 (1998).

[14] A. Asenov and S. Saini, IEEE Trans. Electron Dev., vol. 46, 1718 (1999).

[15] W. J. Gross, D. Vasileska and D. K. Ferry, IEEE Electron Device Lett., vol. 20, 463 (1999).

[16] W. J. Gross, D. Vasileska and D. K. Ferry, IEEE Trans. Electron Dev. (special issue), in press.